ADVANCED FUNCTIONAL MATERIALS
www.afm-journal.de

Structure-Dependent Optical Modulation of Propulsion and Collective Behavior of Acoustic/Light-Driven Hybrid Microbowls

*Songsong Tang, Fangyu Zhang, Jing Zhao, Wael Talaat, Fernando Soto, Emil Karshalev, Chuanrui Chen, Zhihan Hu, Xiaolong Lu, Jinxing Li, Zhihua Lin, Haifeng Dong, Xueji Zhang, Amir Nourhani, and Joseph Wang**

Hybrid light/acoustic-powered microbowl motors, composed of gold (Au) and titanium dioxide (TiO_2) with a structure-dependent optical modulation of both their movement and collective behavior are reported by reversing the inner and outer positions of Au and TiO_2. The microbowl propels in an acoustic field toward its exterior side. UV light activates the photochemical reaction on the TiO_2 surface in the presence of hydrogen peroxide and the Au/TiO_2 system moves toward its TiO_2 side by self-electrophoresis. Controlling the light intensity allows switching of the dominant propulsion mode and provides braking or reversal of motion direction when TiO_2 is on the interior, or accelerated motion when the TiO_2 is on its exterior. Theoretical simulations offer an understanding of the acoustic streaming flow and self-electrophoretic fluid flow induced by the asymmetric distribution of ions around the microbowl. The light-modulation behavior along with the tunable structure also leads to the control of the swarm behaviors under the acoustic field, including expansion or compaction of ensembles of microbowls with interior and exterior TiO_2, respectively. Such structure-dependent motion control thus paves the way for a variety of complex microscale operations, ranging from cargo transport to drug delivery in biomedical and environmental applications.

1. Introduction

Artificial micro/nanomotors have the unique ability to move autonomously or under various external stimuli and perform different complex tasks at small scales,[1] with potential biomedical,[2–6] environmental remediation,[7–9] and energy[10] applications. One of the grand challenges in this field is achieving precise motion control at micro/nanoscales and exploiting[11] or overcoming[12] the effects of random and Brownian motions. The microswimmer structure, the driving forces and the external stimuli are among the key factors for engineering the dynamics of these small-scale motors. Structural properties, such as shape, size, and material composition, can play a central role in micromotor locomotion.[13,14]

Initial studies in the field focused primarily on designing micromotors powered by only one physical (magnetic,[15,16] ultrasound[17–19]) or chemical[20–22] propulsion mechanisms, with limited control over micromotor motion. Building on these pioneering studies, hybrid motors that harvest energy from two power sources and exploit competing driving forces have been developed recently for modulating the dynamics of micromotors and obtaining precise nanoscale motion control, leading to attractive braking, acceleration and direction-reversal capabilities.[23–27]

To date, several hybrid motor designs have successfully integrated dual-powered engines, including chemical/light,[23] magnetic/acoustic,[24] chemical/magnetic,[25] chemical/acoustic[26] controlled operations. Among the different power sources, light is an attractive remote stimulus for generating an effective and extended micro/nanomotor propulsion in connection to variety of photoresponsive materials with different light intensities and wavelengths.[28,29] Acoustic stimulus also attracts a tremendous recent attention due to distinct advantages, including fuel-free, noninvasive, and salt-tolerant motion[19,30] The combination of light and acoustic propulsions holds considerable promise for expanding the scope of hybrid micromotors and for designing advanced microvehicles with adaptive operation in dynamically changing environments. However, to the best of our knowledge, there are no reports on hybrid micromotors powered by ultrasound and light stimuli and on the use of light for controlling and modulating the motion of ultrasound-powered micromotors.

S. Tang, F. Zhang, Prof. J. Zhao, Dr. W. Talaat, F. Soto, E. Karshalev, Dr. C. Chen, Z. Hu, Prof. X. Lu, Dr. J. Li, Z. Lin, Dr. A. Nourhani, Prof. J. Wang
Department of Nanoengineering
University of California San Diego
La Jolla, CA 92093, USA
E-mail: josephwang@ucsd.edu
S. Tang, Prof. H. Dong, Prof. X. Zhang
Research Center for Bioengineering and Sensing Technology
University of Science and Technology Beijing
Beijing 100083, P. R. China
The ORCID identification number(s) for the author(s) of this article can be found under https://doi.org/10.1002/adfm.201809003.

DOI: 10.1002/adfm.201809003

Here we present an attractive design and operation of light/acoustic hybrid microbowl motors consisting of gold (Au) and titanium dioxide (TiO_2) surfaces, with precise structure-dependent motion control and collective behavior based on the different arrangements and configurations of these materials. The resulting Au/TiO_2 microbowl motor propels toward its exterior side in an acoustic field. In the presence of hydrogen peroxide (H_2O_2) and UV light, the combination of photochemical reaction on the TiO_2 surface and catalytic reaction on the Au side results in self-phoretic motion of the microbowl toward its TiO_2 side. For a microbowl with an internal Au surface and TiO_2 on its exterior, the acoustic-actuated and self-phoretic motions are in the same direction and controlling the light intensity offers acceleration of the microbowl movement. Reversing the position of Au and TiO_2 surfaces to exterior and interior, respectively, leads to competing acoustic and phoretic propulsions modes, with phoretic motion toward the interior TiO_2 surface. The propulsion force can be tuned by changing the light intensities or ultrasound transducer voltage, enabling dynamic switching of the dominant propulsion mode and hence leading to light-induced braking action and reversal of the motion direction. Moreover, these structure-dependent optical modulations enable on-demand regulations of the collective behavior, including expansion or compaction, for ensembles of different microbowl structures. Such new design with advanced hybrid operations—including speed tuning (braking and acceleration) capabilities, along with reversed directionality—could expand the scope of micromotor manipulation and provide an attractive route for achieving precise control of micromachines.

2. Results and Discussion

The fabrication process of the microbowls is illustrated in **Figure 1**A and described in detail in the Experimental Section. A microbowl composed of interior TiO_2 (Au) and exterior Au (TiO_2) surfaces is named TiO_2–Au (Au–TiO_2) microbowl. The scanning electron microscope (SEM) and energy-dispersive X-ray (EDX) images for both kinds of microbowls are displayed in Figure S1 (Supporting Information), demonstrating the formation of the bowl-like structure and TiO_2 layer after calcination.

The theoretical simulation in Figure 1F shows flow field (in the particle reference frame) due to the acoustic propulsion of the microbowl toward its exterior. The acoustic propulsion mechanism is based on second-order acoustic streaming flow due to the oscillations of the sharp edges[19] and is independent of Au or TiO_2 positions in a microbowl.[17] For small edge oscillation amplitude ε compared to the particle radius a in an oscillating acoustic field, we can expand the fluid velocity in terms of ε/a, in the form $\boldsymbol{u} = (\varepsilon/a)\,\boldsymbol{u}^{(1)} + (\varepsilon/a)^2\boldsymbol{u}^{(2)} + \mathcal{O}[(\varepsilon/a)^3]$. The first order term $\boldsymbol{u}^{(1)}$ follows a Stokes equation and is oscillatory with the same frequency of the acoustic field. The inertial term $\langle \boldsymbol{u}^{(1)} \cdot \nabla \boldsymbol{u}^{(1)} \rangle$, averaged over one period of oscillation, serves as a body force for Stokes equation governing the second order term averaged over one oscillation period, $\langle \boldsymbol{u}^{(2)} \rangle$. The acoustic streaming is indeed the steady-state velocity field $\langle \boldsymbol{u}^{(2)} \rangle$ and is second order in the amplitude of oscillation $(\varepsilon/a)^2$. Similar phenomena are observed in other microswimmer systems driven by oscillation of a sharp edge in an acoustic field.[19] The light activated self-phoretic motion upon UV illumination in the H_2O_2 solution is toward the TiO_2 side for each kind of microbowl, as illustrated by theoretical simulations in Figure 1G,H. The Au/TiO_2 structure in the presence of hydrogen peroxide and UV light behaves like an electrochemical cell and follows these reactions:

$$TiO_2 + h\nu \rightarrow TiO_2\left(e^- + h^+\right) \quad (1)$$

$$H_2O_2 + 2h^+ \xrightarrow{TiO_2} 2H^+ + O_2 \quad (2)$$

$$H_2O_2 + 2H^+ + 2e^- \xrightarrow{Au} 2H_2O \quad (3)$$

The UV light energy of 3.4 eV (wavelength 365 nm) is within the band gap range of anatase TiO_2 thin films,[31] thus excites an electron e^- to the conduction band and leaves behind a positive hole h^+ in the valence band, as noted in Equation (1). Then, the hydrogen peroxide is decomposed into oxygen molecule and hydrogen ions (Equation (2)) in a half-anodic reaction on the TiO_2 surface.[32] The half-cathodic reaction occurs on the Au surface[33] where the hydrogen ions are consumed. (Equation (3)) The production of hydrogen ion on the TiO_2 surface and its consumption on the Au surface lead to an asymmetric distribution of ions around the microbowl, which drives the micromotor to undergo self-phoretic propulsion[22,28,34–39] toward the TiO_2 side.

To model this mechanism we considered the normal component of the hydrogen ion flux to be positive on the TiO_2 surface and negative on the gold side while the flux of negative ions all over the particle surface is zero. Also, since TiO_2 has excited electrons in the conduction band in the presence of UV light, we approximated the particle surface to be equipotential to leading order in Debye length, an approximation used for bimetallic systems.[37] Then, by solving the coupled set of Stokes equation, Poisson equation and continuity equations of mass and ions, we obtain the flow field around the particle in the particle frame of reference, as shown in Figure 1G,H, which verifies the proposed mechanism for experimental observations.

The simulation results (Figure 1G,H) are in the particle reference frame and the flow field is toward the TiO_2 side. Thus, in the laboratory reference frame (experimental observation under microscope), the direction of the microbowl motion is toward its TiO_2 side. The hydrogen ions produced on the TiO_2 surface diffuse toward the gold side where they are consumed. During the diffusion process, the ions pull the water molecules toward the gold side, giving momentum to the fluid, and resulting in microflow around the microbowl.[37]

We take advantage of the contributions from acoustic and self-phoretic propulsion mechanisms to tune and modulate the microbowl motion, depending on its structure. Both types of microbowls (Au–TiO_2 and TiO_2–Au) are propelled toward their exterior surface under the acoustic field. For the TiO_2–Au microbowl, subsequent illumination of UV light generates a competing self-phoretic propulsion toward the interior TiO_2 side, opposite to the acoustic propulsion. The net outcome of these competing driving forces determines the direction of

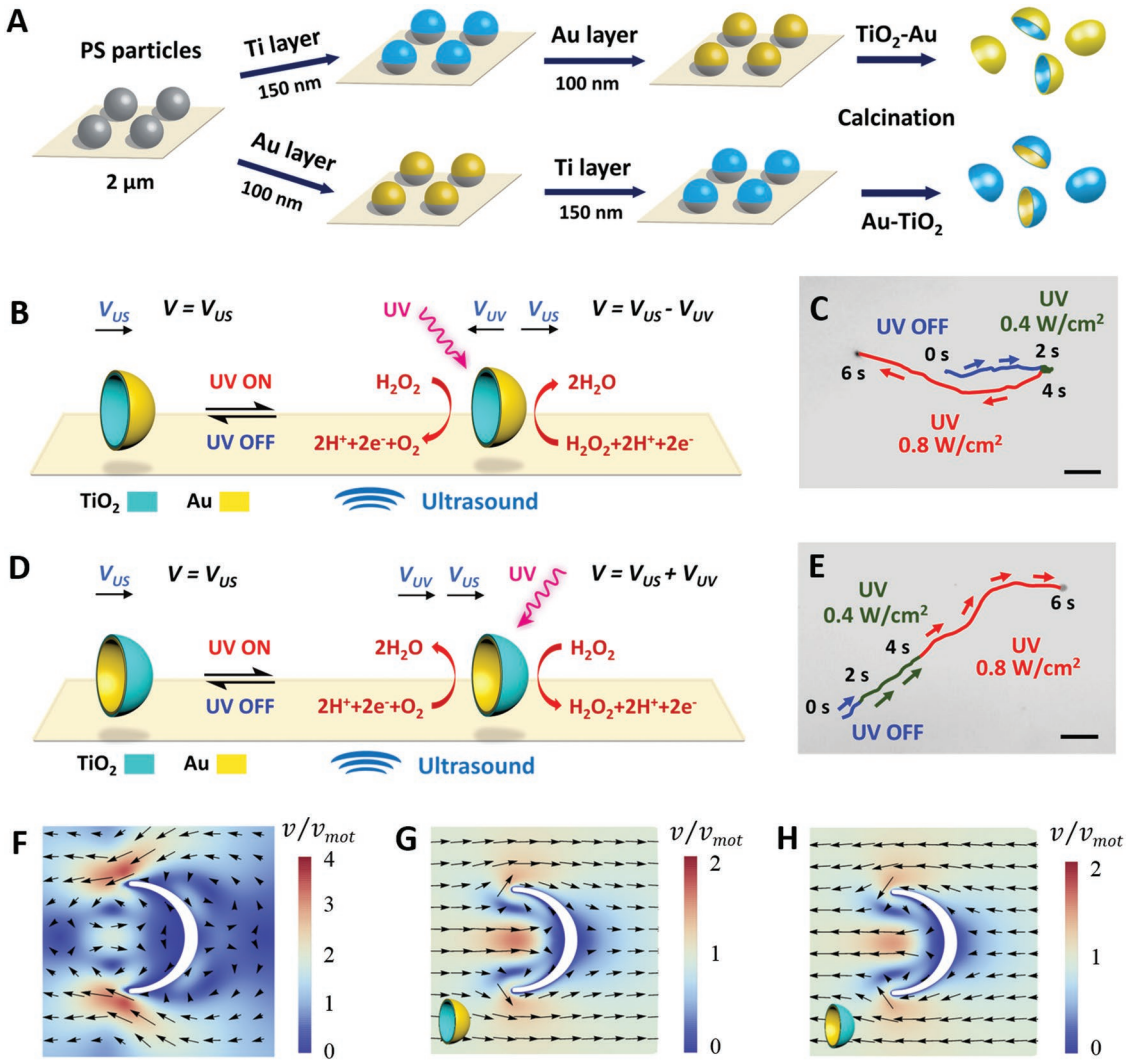

Figure 1. Fabrication process and mechanisms of structure-dependent optical modulations of TiO_2–Au and Au–TiO_2 microbowls under the acoustic field. A) Schematic illustration of the fabrication process of light/acoustic-powered hybrid microbowls. Schematic illustration of structure-dependent optical modulation of B) a TiO_2–Au and D) an Au–TiO_2 microbowl motion under the acoustic field. C) Continuous control of optical braking and motion direction reversal of a TiO_2–Au microbowl in an acoustic field (2.66 MHz, 5 V) (Video S1, Supporting Information). E) Continuous control of optical acceleration of an Au–TiO_2 microbowl in an acoustic field (2.66 MHz, 2.5 V) (Video S2, Supporting Information). Conditions: 10% H_2O_2 solution. Theoretical simulations of F) acoustic streaming flow around the microbowl in acoustic field, and G,H) fluid flow induced by the asymmetric distribution of hydrogen ion around the TiO_2–Au and Au–TiO_2 microbowls under UV illumination, respectively. Scale bars: 10 μm.

the motion and allows the switching of the dominant propulsion mode by changing the light intensity (Figure 1B). Such micromotors obtain precise control by exploiting the competing driving forces, to offer optical braking and reversed directionality capabilities. On the other hand, the acoustic and self-phoretic propulsion modes of the Au–TiO_2 microbowl are in the same direction toward the exterior TiO_2 surface, resulting in increased light-modulated speed (Figure 1D).

The experimental observations of trajectories for these structure-dependent light modulations are demonstrated in Figure 1C, E. All the experiments in this study are performed in a 10% H_2O_2 solution. The acoustic propulsion is defined as a "forward" (positive) motion. The acoustic frequency for single particle propulsion experiments is 2.66 MHz, and for swarming experiments is 618 kHz (Figure 4). The acoustic propulsion speed and self-phoretic speed change linearly with the applied voltage and light intensity, respectively, as shown in Figure S2 and described in detail in the Supporting Information. The micromotor trajectories, as shown in Figure 1C and Video S1 in the Supporting Information, illustrate light induced optical braking and reversal of the motion direction of the TiO_2–Au microbowl under an acoustic field. The acoustic-powered TiO_2–Au microbowl moves at a speed of 11.35 μm s^{-1} during the initial 2 s (blue track line). Upon UV exposure (0.4 W cm^{-2}), the green track line reveals a shorter distance reflecting the immediate speed diminution to 5.1 μm s^{-1} (2–4 s period) associated with the competing driving forces. Increasing the light intensity further to 0.8 W cm^{-2} resulted in reversal of the motion direction with a speed of 21.8 μm s^{-1} (4–6 s). In this case, the light propulsion dominates the acoustic one due to the

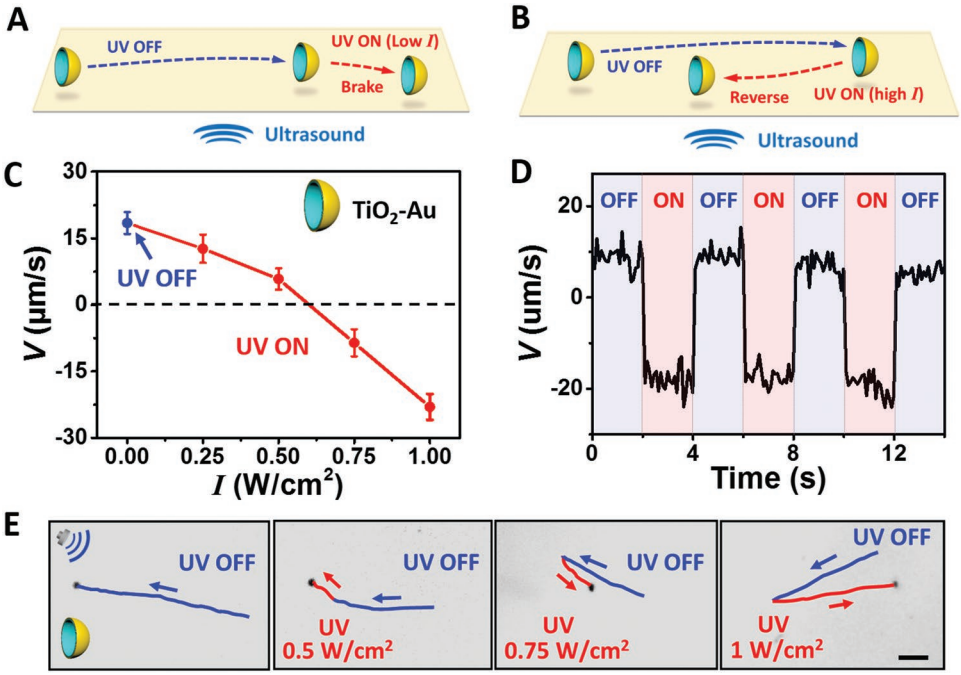

Figure 2. Light-modulated motion control of TiO_2–Au microbowls under the acoustic field. Scheme of light-modulated motion control, including A) optical braking and B) reversed direction of TiO_2–Au microbowls under acoustic field. C) Speed profile and E) corresponding trajectories over 3 s (from Video S3 in the Supporting Information) of TiO_2–Au microbowls upon different light intensities from 0.25 to 1 W cm^{-2} under acoustic field (2.66 MHz, 8 V). Scale bars: 10 μm. D) Speed changes, with the light modulation (0.75 W cm^{-2}) over 2 s, of a typical TiO_2–Au microbowl under acoustic field (2.66 MHz, 2.5 V) (from Video S5 in the Supporting Information). Condition: 10% H_2O_2 solution.

enhanced photochemical reaction on the TiO_2 surface. On the other hand, the continuous light-triggered acceleration of the Au–TiO_2 microbowl under the acoustic field (2.66 MHz, 2.5 V) is also demonstrated in Figure 1E (Video S2, Supporting Information). The Au–TiO_2 microbowl initially moves acoustically at a speed of 5.2 μm s^{-1} (0–2 s period), followed illumination of the UV light that leads to higher speeds of 14.6 and 25.3 μm s^{-1} using light intensities of 0.4 and 0.8 W cm^{-2} during the 2–4 s and 4–6 s periods, respectively. Such response to the light stimulus and precise real-time modulation of the speed and direction of acoustic-powered microbowls depend on the exact positions of Au and TiO_2 surfaces on the bowl structure.

Figure 2A,B illustrates the optical control of ultrasound-powered TiO_2–Au microbowls. As shown in Figure 2C, the average speed of TiO_2–Au microbowls under ultrasound mode (2.66 MHz, 8 V) is 18.5 μm s^{-1}. Subsequent application of UV light induces average velocity reduction from 18.5 to −23.0 μm s^{-1} upon increasing light intensity from 0 to 1 W cm^{-2}. Switching the dominant driving mode from acoustic to optical by increasing the UV intensity can induce an optical brake and reversal of the motion direction. Figure 2E shows trajectories of acoustic-driven microbowls, taken from Video S3 in the Supporting Information, under different light intensities. The length changes in the red track line shows braking and direction reversal over a 1.5 s UV illumination. As shown in Figure S3 (Video S4, Supporting Information), the TiO_2–Au microbowl moves toward the exterior concave surface in an acoustic field. Upon UV illumination, the motion direction is reversed and the microbowl moves toward its concave interior. No reorientation of the microbowl is observed when UV light is turned on, confirming the scheme of Figure 2A,B. Figure 2D (Video S5, Supporting Information) displays the instantaneous dynamic speed changes of the TiO_2–Au microbowl, between 7.52 and −17.65 μm s^{-1}, observed upon switching the UV light on/off (0.75 W cm^{-2}, every 2 s) under acoustic field (2.66 MHz, 2.5 V). Such behavior reflects the rapid response to the light stimulus and the highly repeatable optical control of TiO_2–Au microbowls.

On the other hand, **Figure 3**A illustrates the optical acceleration of Au–TiO_2 microbowls under acoustic field. The effect of the light intensity upon the speed of the microbowl is shown in Figure 3B. The acoustic-driven (2.66 MHz, 5 V) microbowl moves at an average speed of 11.9 μm s^{-1}. Upon UV illumination, the Au–TiO_2 maintains the same movement direction, but accelerates its speed from 11.9 to 39.5 μm s^{-1} over the 0 to 1 W cm^{-2} light intensity range. The red trajectories over 1.5 s in Figure 3D (taken from Video S6 in the Supporting Information) get longer upon increasing the light intensity, consistent with the light-modulated acceleration behavior. The ability to control multiple microbowls under UV light (0.75 W cm^{-2}) is demonstrated in Video S7 in the Supporting Information. The reproducibility of such speed increase is illustrated in Figure 3C (and Video S8 in the Supporting Information), which exhibit the periodic speed changes between the average speed of 6.46 and 26.42 μm s^{-1} upon repeated UV "On" and "Off" cycles (0.75 W cm^{-2}, every 2 s) under acoustic field (2.66 MHz, 2.5 V). Overall, these data further demonstrate that by changing the position of TiO_2 to interior or exterior, we can reverse the direction of the light propulsion, or maintain the same direction as the acoustic propulsion, respectively, leading to the structure-dependent optical

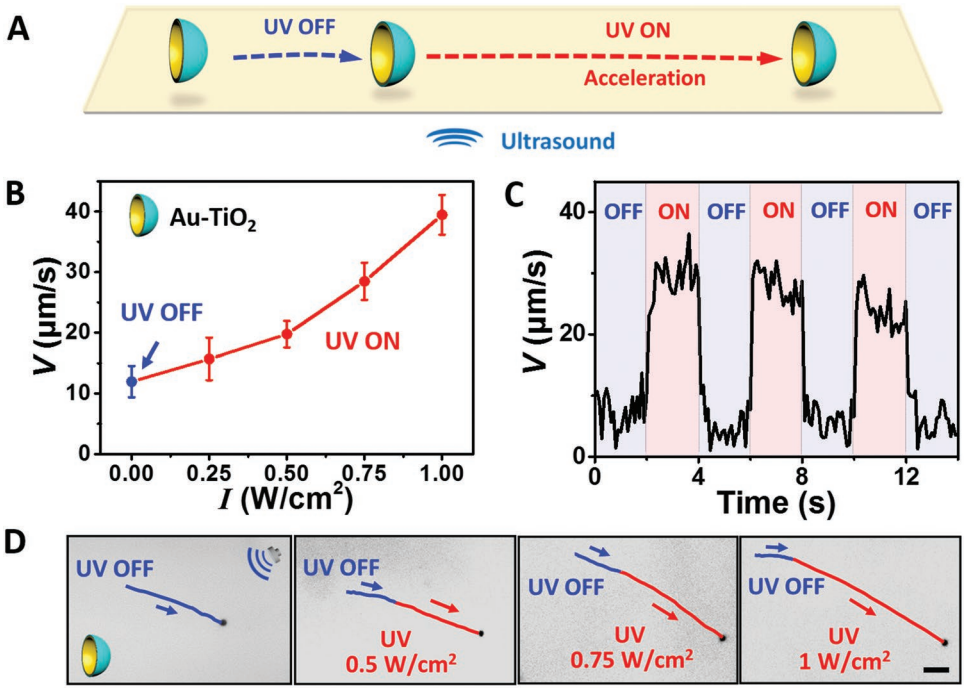

Figure 3. Light-modulated motion control of Au–TiO_2 microbowls under the acoustic field. A) Scheme of light-based acceleration of the acoustically propelled Au–TiO_2 microbowl. B) Speed profile and D) corresponding trajectories over 3 s (Video S6, Supporting Information) of Au–TiO_2 microbowls using different light intensities from 0.25 to 1 W cm^{-2} under acoustic field (2.66 MHz, 5 V). Scale bars: 10 μm. C) Dynamic speed changes of the Au–TiO_2 microbowls upon turning the light off and on (0.75 W cm^{-2}) using 2 s intervals under acoustic field (2.66 MHz, 2.5 V) (Video S8, Supporting Information). Condition: 10% H_2O_2 solution.

modulation with instantaneous, programmable and reproducible speed and direction regulations.

Collective behavior in micromotors, including previously reported aggregation, dispersion and migration,[24,40–43] has motivated us to explore the swarm behaviors of hybrid microbowls in response to optical stimuli. Aggregates of the two different microbowl structures have displayed opposite response to UV light under acoustic field (618 kHz). As illustrated in **Figure 4**, aggregates of TiO_2–Au and Au–TiO_2 microbowls are formed by the migration of microbowls to low-pressure regions (nodes) in an acoustic pressure gradient.[44] Upon UV illumination, TiO_2–Au microbowls move away from the node center, leading to the expansion of the assembly (Figure 4C). In contrast, the aggregate of Au–TiO_2 microbowls exhibits an opposite response to the UV light, resulting in a tighter aggregate (Figure 4D). Such swarm behaviors can be dynamically repeated by switching UV light on and off, as illustrated in Figure 4C (Video S9, Supporting Information) and Figure 4D (Video S10, Supporting Information).

The corresponding area change ratios ($\Delta A/A_0$) of resulting swarm are shown in Figure 4E,F. Using TiO_2–Au microbowls the aggregate area increases rapidly initially upon illuminating UV light (between 0.5 and 3.1 s), followed by a significant decrease upon turning the UV light off (between 3.1 and 10 s). In contrast, using the Au–TiO_2 microbowls the change in the aggregate area upon the UV illumination is negligible, since the light driven motion is toward the node and the aggregate is already almost packed. Such light modulated structure-dependent expansion and compaction of TiO_2–Au and Au–TiO_2 microbowl ensembles, respectively, is highly reversible and repeatable and hold promise for assembling and controlling groups of micromachines for performing cooperative tasks.

Here we elaborate on the underlying mechanisms of the aforementioned observations. The acoustic force aggregates the particle at the node regardless of the micromotor structure, as was described previously. We attribute this unique behavior to the aggregation of the particle population with their exterior pointed toward the center of the assembly, as illustrated in the idealized scheme of Figure 4. Upon UV illumination, the particles with interior TiO_2 try to move away from the aggregate against the acoustic force, thus leading to expanded aggregate. The heterogeneous distribution of the particle orientation within the aggregate before the UV stimulation results in the formation of small island in the expanded aggregate. On the other hand, particles with exterior TiO_2 surface, tend to move further toward the center upon UV illumination, thus squeezing the aggregation. However, since the aggregate is already highly packed, the compression of the population is small.

3. Conclusions

In conclusion, we have presented the first example of light-acoustic powered hybrid microbowls with structure-dependent light modulated motion control and collective behavior. The acoustic streaming flow generated by the oscillation of a microbowl propels the motor toward its exterior

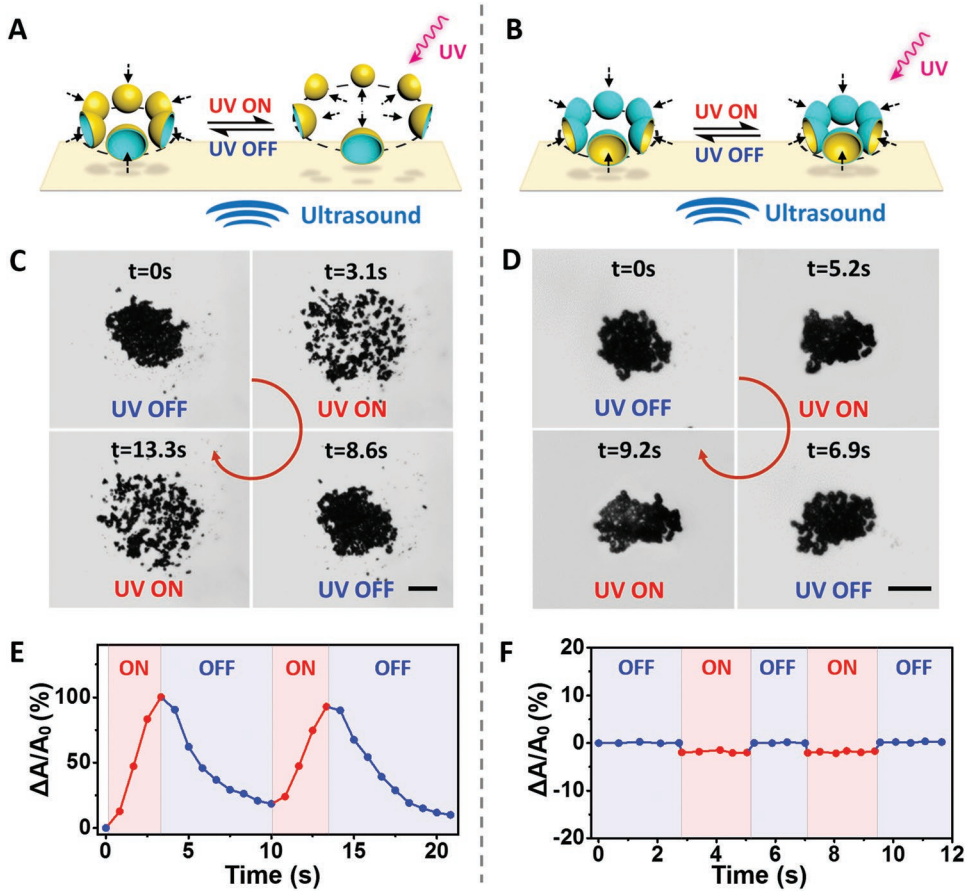

Figure 4. Structure-dependent optical modulation of collective behavior under the acoustic field. Schematic illustration, snapshots, and area change ratio of A,C,E) dispersion behavior of resulting swarm of TiO_2–Au microbowls (Video S9, Supporting Information) and B,D,F) compaction of resulting swarm of Au–TiO_2 microbowls upon UV illumination (Video S10, Supporting Information), respectively. Scale bar: 20 µm. Conditions: 10% H_2O_2 solution. US: 618 kHz, 1.5 V for TiO_2–Au microbowls, and 5 V for Au–TiO_2 microbowls. UV: 1 W cm^{-2}.

concave surface. The micromotor thus moves toward the TiO_2 side in the presence of UV light and hydrogen peroxide. The light-driven propulsion is in the same or opposite directions of the acoustic-actuated propulsion, depending if the TiO_2 is on the external or internal side of the microbowl, respectively. A dramatically modulated swimming behavior has thus been realized by tuning the geometry and light intensity. An attractive structure-dependent light modulation of the acoustic motion can thus be achieved, including optical braking, direction reversal for TiO_2–Au microbowls, or accelerated motion for the Au–TiO_2 microbowls. Future efforts will lead to advanced microvehicles integrating these capabilities into a single vehicle structure and toward migration of hybrid micromotor swarms. Structure-dependent expansion or compaction of microbowls ensembles, triggered by UV light, are observed under an acoustic field. The optical modulation of the motor dynamics is rapid, repeatable and reversible. The new structure-dependent hybrid operations and tunable motion control pave the way to advanced microvehicles with precise manipulation and adaptive performance under dynamically changing environments toward diverse applications ranging from microscale fabrication to microchip operations.

4. Experimental Section

Synthesis of TiO_2–Au and Au–TiO_2 Microbowls: The fabrication process is illustrated in Figure 1A. Polystyrene beads (PS, 2 µm, Polysciences, Inc.) were first dispersed over a glass slide as the template. Metallic bilayers composed of a titanium layer (150 nm) and a gold layer (100 nm) were deposited on the beads by Temescal BJD 1800 E-beam evaporator. The obtained Janus microparticles were calcined at 450 °C for 3 h to get the anatase TiO_2 layer[36,39] and simultaneously remove PS template, resulting in bowl-shaped micromotors. Switching the deposition sequence of Au and Ti leads to two kinds of final products, TiO_2–Au and Au–TiO_2 microbowls.

Equipment: The ultrasound equipment is described in previous report.[17] An inverted optical microscope, Nikon Eclipse 80i, coupled to a 20× objective, a Photometrics CoolSnap HQ2 CCD camera and MetaMorph 7.6 software (Molecular Devices, Sunnyvale, CA) were used to capture videos, which were analyzed by NIS-Elements AR 3.2 and ImageJ software. SEM and EDX analyses were carried out on an Apreo high resolution instrument (FEI, Hillboro, Oregon, USA) with an acceleration voltage of 10 kV. UV lamp (365 nm) was purchased from Shenzhen Lamplic Technology Company. All the experiments are performed in 10% H_2O_2 solution (Sigma Aldrich).

Supporting Information

Supporting Information is available from the Wiley Online Library or from the author.

Acknowledgements

S.T., F.Z., and J.Z. contributed equally to this work. This work was supported by grants from the Defense Threat Reduction Agency Joint Science and Technology Office for Chemical and Biological Defense (Grant No. HDTRA1-14-1-0064). S.T. and J.Z. acknowledge the China Scholarship Council (CSC) for the financial support. W.T. and F.S. acknowledge the Egypt Missions and UC MEXUS-CONACYT, respectively, for financial support. E.K. acknowledges support from the Charles Lee Powell Foundation.

Conflict of Interest

The authors declare no conflict of interest.

Keywords

collective behavior, composite microbowl, light/acoustic hybrid propulsion, optical modulation, self-propelling micromotor

Received: December 18, 2018
Revised: February 25, 2019
Published online: April 5, 2019

[1] J. Wang, *Nanomachines: Fundamentals and Applications*, Wiley-VCH, Weinheim, Germany **2013**.
[2] J. Li, B. Esteban-Fernández de Ávila, W. Gao, L. Zhang, J. Wang, *Sci. Robot.* **2017**, *2*. eaam6431.
[3] B. Esteban-Fernández de Ávila, W. Gao, E. Karshalev, L. Zhang, J. Wang, *Acc. Chem. Res.* **2018**, *51*, 1901.
[4] X. Lin, Z. Wu, Y. Wu, M. Xuan, Q. He, *Adv. Mater.* **2016**, *28*, 1060.
[5] Z. Wu, X. Lin, T. Si, Q. He, *Small* **2016**, *12*, 3080.
[6] K. Kim, J. Guo, Z. Liang, D. Fan, *Adv. Funct. Mater.* **2018**, *28*, 1705867.
[7] J. Parmar, D. Vilela, K. Villa, J. Wang, S. Sanchez, *J. Am. Chem. Soc.* **2018**, *140*, 9317.
[8] W. Gao, J. Wang, *ACS Nano* **2014**, *8*, 3170.
[9] M. Safdar, S. U. Khan, J. Janis, *Adv. Mater.* **2018**, *30*, 1703660.
[10] V. V. Singh, F. Soto, K. Kaufmann, J. Wang, *Angew. Chem., Int. Ed.* **2015**, *127*, 7000.
[11] A. Nourhani, V. H. Crespi, P. E. Lammert, *Phys. Rev. Lett.* **2015**, *115*, 118101.
[12] S. Das, A. Garg, A. I. Campbell, J. Howse, A. Sen, D. Velegol, R. Golestanian, S. J. Ebbens, *Nat. Commun.* **2015**, *6*, 8999.
[13] S. Ahmed, W. Wang, L. Bai, D. T. Gentekos, M. Hoyos, T. E. Mallouk, *ACS Nano* **2016**, *10*, 4763.
[14] X. Ma, S. Jang, M. N. Popescu, W. E. Uspal, A. Miguel-Lopez, K. Hahn, D. P. Kim, S. Sanchez, *ACS Nano* **2016**, *10*, 8751.
[15] S. Tottori, L. Zhang, F. Qiu, K. K. Krawczyk, A. Franco-Obregon, B. J. Nelson, *Adv. Mater.* **2012**, *24*, 811.
[16] J. Li, S. Sattayasamitsathit, R. Dong, W. Gao, R. Tam, X. Feng, S. Ai, J. Wang, *Nanoscale* **2014**, *6*, 9415.
[17] F. Soto, G. L. Wagner, V. Garcia-Gradilla, K. T. Gillespie, D. R. Lakshmipathy, E. Karshalev, C. Angell, Y. Chen, J. Wang, *Nanoscale* **2016**, *8*, 17788.
[18] D. Ahmed, M. Lu, A. Nourhani, P. E. Lammert, Z. Stratton, H. S. Muddana, V. H. Crespi, T. J. Huang, *Sci. Rep.* **2015**, *5*, 9744.
[19] M. Kaynak, A. Ozcelik, A. Nourhani, P. E. Lammert, V. H. Crespi, T. J. Huang, *Lab Chip* **2017**, *17*, 395.
[20] W. F. Paxton, K. C. Kistler, C. C. Olmeda, A. Sen, S. K. St. Angelo, Y. Cao, T. E. Mallouk, P. E. Lammert, V. H. Crespi, *J. Am. Chem. Soc.* **2004**, *126*, 13424.
[21] R. Laocharoensuk, J. Burdick, J. Wang, *ACS Nano* **2008**, *2*, 1069.
[22] A. Nourhani, P. E. Lammert, *Phys. Rev. Lett.* **2016**, *116*, 178302.
[23] C. Chen, S. Tang, H. Teymourian, E. Karshalev, F. Zhang, J. Li, F. Mou, Y. Liang, J. Guan, J. Wang, *Angew. Chem., Int. Ed.* **2018**, *57*, 8110.
[24] J. Li, T. Li, T. Xu, M. Kiristi, W. Liu, Z. Wu, J. Wang, *Nano Lett.* **2015**, *15*, 4814.
[25] W. Gao, K. M. Manesh, J. Hua, S. Sattayasamitsathit, J. Wang, *Small* **2011**, *7*, 2047.
[26] L. Ren, D. Zhou, Z. Mao, P. Xu, T. J. Huang, T. E. Mallouk, *ACS Nano* **2017**, *11*, 10591.
[27] C. Chen, F. Soto, E. Karshalev, J. Li, J. Wang, *Adv. Funct. Mater.* **2018**, 1806290.
[28] L. Xu, F. Mou, H. Gong, M. Luo, J. Guan, *Chem. Soc. Rev.* **2017**, *46*, 6905.
[29] R. Dong, Y. Cai, Y. Yang, W. Gao, B. Ren, *Acc. Chem. Res.* **2018**, *51*, 1940.
[30] Y. Tu, F. Peng, D. A. Wilson, *Adv. Mater.* **2017**, *29*, 1701970.
[31] Z. Wang, U. Helmersson, P.-O. Käll, *Thin Solid Films* **2002**, *405*, 50.
[32] J. Yi, C. Bahrini, C. Schoemaecker, C. Fittschen, W. Choi, *J. Phys. Chem. C* **2012**, *116*, 10090.
[33] Y. Wang, R. M. Hernandez, D. J. Bartlett, J. M. Bingham, T. R. Kline, A. Sen, T. E. Mallouk, *Langmuir* **2006**, *22*, 10451.
[34] W. Wang, W. Duan, S. Ahmed, T. E. Mallouk, A. Sen, *Nano Today* **2013**, *8*, 531.
[35] R. Dong, Q. Zhang, W. Gao, A. Pei, B. Ren, *ACS Nano* **2016**, *10*, 839.
[36] F. Mou, L. Kong, C. Chen, Z. Chen, L. Xu, J. Guan, *Nanoscale* **2016**, *8*, 4976.
[37] A. Nourhani, V. H. Crespi, P. E. Lammert, A. Borhan, *Phys. Fluids* **2015**, *27*, 092002.
[38] A. Nourhani, P. E. Lammert, V. H. Crespi, A. Borhan, *Phys. Fluids* **2015**, *27*, 012001.
[39] C. Chen, F. Mou, L. Xu, S. Wang, J. Guan, Z. Feng, Q. Wang, L. Kong, W. Li, J. Wang, Q. Zhang, *Adv. Mater.* **2017**, *29*, 1603374.
[40] T. Xu, F. Soto, W. Gao, R. Dong, V. Garcia-Gradilla, E. Magana, X. Zhang, J. Wang, *J. Am. Chem. Soc.* **2015**, *137*, 2163.
[41] D. Zhou, Y. Gao, J. Yang, Y. C. Li, G. Shao, G. Zhang, T. Li, L. Li, *Adv. Sci.* **2018**, *5*, 1800122.
[42] Y. Zhang, K. Yan, F. Ji, L. Zhang, *Adv. Funct. Mater.* **2018**, *28*, 1806340.
[43] J. Yu, B. Wang, X. Du, Q. Wang, L. Zhang, *Nat. Commun.* **2018**, *9*, 3260.
[44] T. Laurell, F. Petersson, A. Nilsson, *Chem. Soc. Rev.* **2007**, *36*, 492.